Microstructural Parameters in Electron-Irradiated C108 Silk Fibers by Wide-Angle X-Ray Scattering Studies

Sangappa,[1] S. Asha,[1] Ganesh Sanjeev,[2] G. Subramanya,[3] P. Parameswara,[4] R. Somashekar[4]

[1]*Department of Studies in Physics, Mangalore University, Mangalagangotri 574 199, India*
[2]*Microtron Center, Mangalore University, Mangalagangotri 574 199, India*
[3]*Department of Studies in Sericulture, University of Mysore, Manasagangotri, Mysore 570 006, India*
[4]*Department of Studies in Physics, University of Mysore, Manasagangotri, Mysore 570 006, India*

Received 22 January 2009; accepted 16 August 2009
DOI 10.1002/app.31312
Published online 7 October 2009 in Wiley InterScience (www.interscience.wiley.com).

ABSTRACT: The present study looks into the microstructural changes in C108 (*Bombyx mori*) silk fibers, induced by electron irradiation. The irradiation process was performed in air at room temperature by the use of 8 MeV electron accelerators at different doses: 0, 25, 50, 75, and 100 kGy, respectively. The changes in microstructural parameters in these natural polymer fibers have been studied using wide-angle X-ray scattering method. The crystal imperfection parameters such as crystallite size $\langle N \rangle$, lattice strain (g in %), and enthalpy (α^*) have been determined by line profile analysis using Fourier method of Warren. Exponential, lognormal, and Reinhold functions for the column length distributions have been used for the determination of these parameters. © 2009 Wiley Periodicals, Inc. J Appl Polym Sci 115: 2183–2189, 2010

Key words: irradiation; microstructural parameters; WAXS; fiber

INTRODUCTION

Silk proteins are of practical interest because of their excellent intrinsic properties useable in biotechnological and biomedical fields as well as the importance of silkworm in the manufacture of textiles.[1] It is quite important to know the microstructural changes in silk fibers due to electron irradiation as these parameters determine the property and strength of the fibers. Such studies have not been carried out except for the chemical effects on these fibers.[2–8] Okuyama et al.[9] have reported crystal structure for silk-I and silk-II fibers. Somashekar et al.[10] have reported the effect of degumming and dye processing on the microstructural parameters in pure Mysore silk, Nistari, NB7, and NB18 silk fibers. Sangappa et al.[11–13] have reported microstructural parameters in hosa Mysore (HM), pure Mysore silk (PMS), Nistari, and C-nichi silk fibers. Takeshita et al.[14] have studied the effect of electron beam irradiation on silk fibers. Effects of gamma irradiation on biodegradation of *Bombyx mori* silk fibers have been performed by Kojthung et al.[15]

When a polymer is subjected to irradiation by ionizing radiation such as gamma rays, X-rays, or accelerated electrons various effects like modification and degradation are expected from the interaction of beam with polymer. At the microscopic level, the polymer degradation is characterized by macromolecular chain splitting, creation of low mass fragments, production of free radicals, oxidation, and crosslinking. These affects the macroscopic properties like mechanical strength, color, electrical conductivity, and so on.[16] The resulting change in the properties of the polymer may extend the range of applications for the material. In radiation chemistry, polymers are classified into two types: scission polymers and crosslinking polymers, in which most biopolymers are classified as scission polymers.[17] The interaction of electron beam with matter results in changes in crystallinity and microstructure. Information obtained from crystallite size and lattice strain analysis can be related to a particular treatment of the materials. Here we have irradiated silk fiber samples with 8 MeV electron beams of various doses. Line profile analysis (LPA) of Bragg's reflections from such irradiated samples is therefore useful for research, development, quality control, and also for understanding the physical, mechanical, and chemical properties which are strongly related to microstructural constituent of the material. Hence in this article we report X-ray profile analysis of Bragg's reflections observed in virgin and electron irradiated C108 silk fibers.

Correspondence to: Sangappa (sangappa@mangaloreuniversity.ac.in).

Contract grant sponsor: University Grant Commission, New Delhi, Govt of India; contract grant number: 33-14/2007.

EXPERIMENTAL

Sample preparation

For our study, we have used raw C108 silk fiber belonging to *Bombyx mori* family which comes under the classification multivoltine on the basis of shape, color, denier, and life cycle of the fibers/cocoons. Cocoons were collected from the germplasm stock of the Department of Sericulture, University of Mysore, India, which were then cooked in boiling water (100°C) for 2 min to soften the sericin and transferred to water bath at 65°C for 2 min. Then the cocoons were reeled in warm water with the help of mono cocoon reeling equipment EPPROUVITE. The characteristic features of these fibers are that they are white in color with an average filament length of 350 m and denier being in the range of 1.8–2.0. These fibers were mounted on rectangular frame in just taut condition which does not involve any mechanical stretching of fibers. The whole process, starting from reeling to mounting of fibers, does not involve any type of mechanical deformation.

Electron irradiation

Irradiation of samples was carried out at Microtron Center; Mangalore University by using the electron beam (by lanthanum hexa fluorite source). The monochromatic beam is made to fall on samples kept at a particular distance with the following beam features (Table I). The dose delivered to different samples is measured by keeping alanine dosimeter with sample during irradiation.

X-ray diffraction measurements

The XRD diffractograms of the fiber samples were recorded using a Rigaku Miniflex-II X-ray diffractometer with Ni filtered, CuKα radiation of wavelength λ = 1.5406 Å, with a graphite monochromator. The scattered beam was focused on a detector. The samples were scanned in the 2θ range 10–50° with a scanning speed and step size of 1° per min and 0.01°, respectively, and the scans are shown in Figure 1.

THEORY

Microstructural parameters such as crystal size $\langle N \rangle$ and lattice strain (g in %) are usually determined by employing Fourier method of Warren and Averbach,[18] and Warren.[19,20] The intensity of a profile in the direction joining the origin to the center of the reflection can be expanded in terms of Fourier cosine series:

$$I(s) = \sum_{n=-\infty}^{\infty} A(n) \cos\{2\pi n d(s - s_0)\} \quad (1)$$

where the coefficients of the harmonics $A(n)$ are functions of the size of the crystallite and the disorder of the lattice. Here, s is sin (θ)/(λ), s_o being the value of s at the peak of a profile, n is the harmonic order of coefficient, and d is the lattice spacing. The Fourier coefficients can be expressed as:

$$A(n) = A_s(n) \times A_d(n) \quad (2)$$

For a paracrystalline material, $A_d(n)$ can be obtained, with Gaussian strain distribution,[21]

$$A_d(n) = exp(-2\pi^2 m^2 n g^2) \quad (3)$$

where "m" is the order of the reflection and $g = (\Delta d/\mathrm{d})$ is the lattice strain. Normally one also defines mean square strain $\langle \varepsilon^2 \rangle$, which is given by g^2/n. This mean square strain is dependent on n, whereas not g.[22,23] For a probability distribution of column lengths $P(i)$, we have:

$$A_s(n) = 1 - \frac{nd}{D} - \frac{d}{D}\left[\int_0^n iP(n)di - n\int_0^n P(i)di\right] \quad (4)$$

where $D = \langle N \rangle d_{hkl}$ is the crystallite size and "i" is the number of unit cells in a column. In the presence of two order of reflections from the same set of Bragg planes, Warren and Averbach[18,19] have shown a method of obtaining the crystal size $\langle N \rangle$ and lattice strain (g in %). But in polymer it is very rare to find multiple reflections. So, to determine the finer details of microstructure, we approximate the size profile by simple analytical function for $P(i)$ by considering only the asymmetric functions. Another advantage of this method is that the distribution function differs along different directions. Whereas, a single size distribution function that is used for the whole pattern fitting, which we feel, may be inadequate to describe polymer diffraction patterns.[22–24] Here it is emphasized that the Fourier method of profile analysis (single order method used here) is quite reliable one as per the recent survey and results of round Robin test conducted by IUCr.[25] In fact, for refinement, we have also considered the effect of background by introducing a parameter [see for details regarding the effect of background on the microcrystalline parameters[26]]. For the sake of completeness, we reproduce the following equations which are used in the computation of microstructural parameters.

THE EXPONENTIAL DISTRIBUTION

It is assumed that there are no columns containing fewer than p unit cells and those with more decay exponentially. Thus, we have,[27]

TABLE I
Specifications of the Electron Beam Accelerator and Irradiation Conditions

1	Beam energy	8 MeV
2	Beam current	20 mA
3	Pulse repetition rate	50 Hz
4	Pulse width	2.2 μs
5	Distance source to sample	30 cm
6	Time of exposure	45 min
7	Dose range	0–100 kGy
8	Atmosphere	Air
9	Temperature	27°C

$$P(i) = \begin{cases} 0 & ; \quad \text{if } p < i \\ \alpha \exp\{-\alpha(i-p)\}; & \text{if } p \geq i \end{cases} \tag{5}$$

where $\alpha = 1/(N - p)$. Substituting this in eq. (4), we get:

$$A_s(n) = \begin{cases} A(0)(1 - n/\langle N \rangle) & ; \quad \text{if } n \leq p \\ A(0)\{\exp[-\alpha(n-p)]\}/(\alpha N); & \text{if } n \geq p \end{cases} \tag{6}$$

where α is the width of the distribution function, "*i*" is the number of unit cells in a column, *n* is the harmonic number, *p* is the smallest number of unit cells in a column and $\langle N \rangle$, the number of unit cells counted in a direction perpendicular to the (*hkl*) Bragg plane.

THE LOGNORMAL DISTRIBUTION

The lognormal distribution function is given by:

$$P(i) = \frac{1}{(2\pi)^{1/2}\sigma}\frac{1}{i}\exp\left\{-\frac{[\log(i/m)]^2}{2\sigma^2}\right\} \tag{7}$$

where σ is the variance and *m* is the median of the distribution function.

Substituting for *P*(*i*) in eq. (4) and simplifying,[5] we get,

$$A_s(n) = \frac{m^3 \exp[(9/4)(2^{1/2}\sigma)^2}{3}\operatorname{erfc}\left[\frac{\log(|n|/m)}{2^{1/2}\sigma} - \frac{3}{2}2^{1/2}\sigma\right] - \frac{m^2 \exp(2^{1/2}\sigma)^2}{2}|n|\operatorname{erfc}\left[\frac{\log(|n|/m)}{2^{1/2}\sigma} - 2^{1/2}\sigma\right] + \frac{|n|^3}{6}\operatorname{erfc}\left[\frac{\log(|n|/m)}{2^{1/2}\sigma}\right] \tag{8}$$

The above equation is the one used by Ribarik et al.[22] The maximal value $A_s(0)$ is given by:

$$A_s(0) = \frac{2m^3 \exp[(9/4)(2^{1/2}\sigma)^2]}{3} \tag{9}$$

The area-weighted number of unit cells in a column is given by

$$\langle N \rangle_{\text{surf}} = \frac{2m \exp[(5/4)(2^{1/2}\sigma)^2]}{3} \tag{10}$$

and the volume-weighted number of unit cell in a column is given by

$$\langle N \rangle_{\text{vol}} = \frac{3m \exp[(7/4)(2^{1/2}\sigma)^2]}{4} \tag{11}$$

THE REINHOLD DISTRIBUTION

With the exponential distribution function, *P*(*i*) rises discontinuously at *p*, from zero to its maximum value. In contrast, the Reinhold function allows a continuous change by putting,

$$P(i) = \begin{cases} 0 & ; \quad \text{if } i \leq p \\ \beta^2(i-p)\exp\{-\beta(i-p)\}; & \text{if } i > p \end{cases} \tag{12}$$

where $\beta = \frac{2}{N-p}$ substituting these in eq. (4), we obtain

$$A_s(n) = \begin{cases} A(0)(1 - n/\langle N \rangle) & ; \quad \text{if } n \leq p \\ [A(0)(n - p + 2/\beta)/N]\{\exp[-\beta(n-p)]\}; & \text{if } n \geq p \end{cases} \tag{13}$$

where β is the width of the distribution which has been varied to fit the experimental results. *p* is the

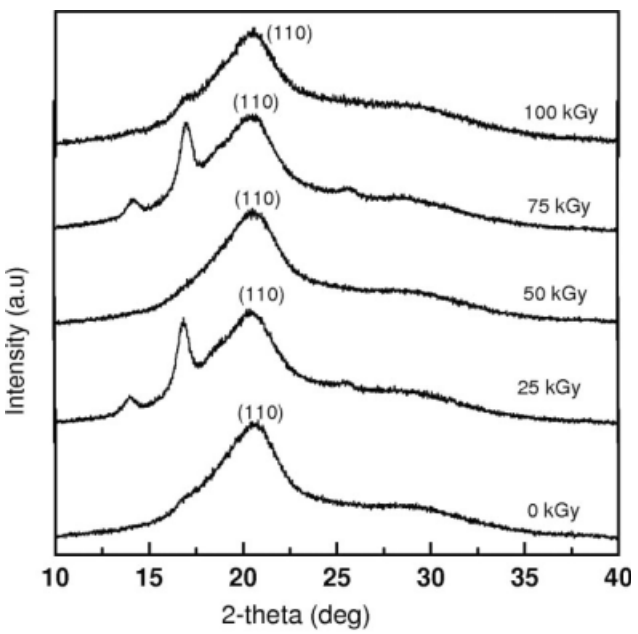

Figure 1 XRD scans of pure and 8 MeV electron irradiated polymer samples.

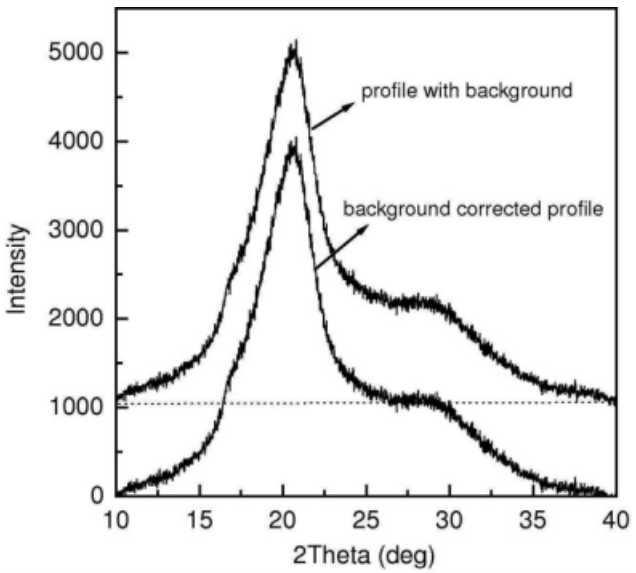

Figure 2 Profiles with background and background corrected C108 silk fiber.

smallest number of unit cells in a column, $\langle N \rangle$ is the number of unit cells counted in a direction perpendicular to the (*hkl*) Bragg plane, d is the spacing of the (*hkl*) planes, λ is the wavelength of X-rays used, i is the number of unit cells in a column, n is the harmonic number, and D_s is the surface weighted crystal size ($\langle N \rangle d_{hkl}$).

All the distribution functions were put to test to find out the most suitable crystal size distribution function for the profile analysis of the X-ray diffraction. The procedure adopted for the computation of the parameters is as follows. Initial values of g and N were obtained using the method of Nandi et al.[28] With these values in the equations give numbers earlier give the corresponding values for the width of distribution. These are only rough estimates, so the refinement procedure must be sufficiently robust to start with such values. Here we compute:

$$\Delta^2 = [I_{\text{cal}} - (I_{\text{exp}} + \text{BG})]^2/\text{npt} \qquad (14)$$

where BG represents the error in the background estimation (Fig. 2), npt is number of data points in a profile, I_{cal} is intensity calculated using eqs. (1)–(13) and I_{exp} is the experimental intensity. The values of Δ were divided by half the maximum value of intensity so that it is expressed relative to the mean value of intensities, and then minimized.

X-ray profile analysis

For the analysis, we have used X-ray diffraction data in the above equations to simulate the intensity profile by varying the necessary parameters till one gets

TABLE II
Microstructural Parameters of Electron Irradiated Polymer Samples Computed by Various Distribution Functions

Sample	Exponential				Reinhold				Lognormal			
	$\langle N \rangle$	g (%)	α^*	D_s (Å)	Delta	$\langle N \rangle$	g (%)	α^*	D_s (Å)	Delta	$\langle N \rangle$	g (%)	α^*	D_s (Å)	Delta
0 kGy	6.95 ± 0.34	0.5 ± 0.02	0.013	29.66	0.049	6.92 ± 0.34	0.2 ± 0.01	0.005	29.53	0.049	7.60 ± 0.46	1.0 ± 0.06	0.028	32.43	0.060
25 kGy	6.52 ± 0.39	0.6 ± 0.04	0.015	28.55	0.061	6.52 ± 0.39	0.4 ± 0.02	0.010	28.55	0.061	7.44 ± 0.45	1.5 ± 0.09	0.041	32.00	0.060
50 kGy	5.63 ± 0.22	0.3 ± 0.01	0.007	24.29	0.038	5.62 ± 0.21	0.5 ± 0.02	0.011	24.26	0.038	5.99 ± 0.29	0.5 ± 0.03	0.012	25.85	0.050
75 kGy	6.01 ± 0.25	0.5 ± 0.02	0.012	25.92	0.041	5.96 ± 0.18	0.5 ± 0.02	0.012	25.69	0.030	6.54 ± 0.39	0.5 ± 0.03	0.013	28.20	0.060
100 kGy	5.83 ± 0.31	0.5 ± 0.02	0.012	25.09	0.053	5.81 ± 0.33	0.5 ± 0.03	0.012	25.00	0.057	6.51 ± 0.52	0.3 ± 0.02	0.008	28.01	0.080

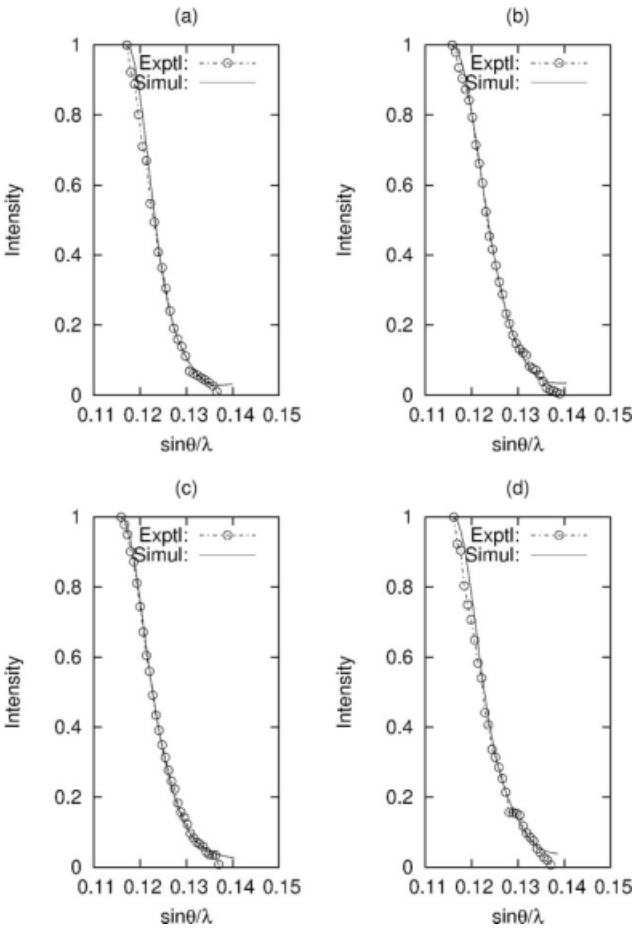

Figure 3 (a–d) Experimental and simulated intensity profiles of X-ray reflection of silk fiber samples obtained with exponential column length distribution function.

a good fit with the experimental profile. For this purpose, a multidimensional algorithm SIMPLEX is used for minimization.[29] We have used pure and 8 MeV electron beam irradiated C108 silk fiber samples. The computed crystal imperfection parameters along with reported physical parameters are given in the Table II for different distribution functions of each of the samples.

RESULTS AND DISCUSSION

Figures 3(a–d) , 4(a–d), and 5(a–d) show the simulated and experimental profiles for 8 MeV electron irradiated and pure polymer samples of Bragg's clear reflections(110) using different asymmetric functions. The simulated profile was obtained with the above equations using appropriate model parameters. This procedure was followed for all the other samples treated at different radiation doses for polymer samples. The computed microcrystalline parameters such as crystallite size $\langle N \rangle$(number of unit cells), lattice strain g in %, the width of the crystallite size distribution (α), and the standard deviation are given in Table II. It is evident from Table II that all the asymmetric distributions used give more or less similar results. By and large, exponential distribution function gives a better fit than Reinhold/log-normal distributions. Here we would like to emphasize that the standard deviation in all the cases for the microstructural parameters are given in Table II as delta. As exponential distribution function gives a better fit than others, we used the corresponding results given in Table II to infer some important conclusions. From the Table II, two important features are to be noted. They are

i. The value of the surface weighted crystallite size D_s (Å) decreases as irradiation dose increases, ii. The value of the crystallite size $\langle N \rangle$ is more for unirradiated polymers.

Irradiation of polymers mainly causes two important changes. (1) Degradation of the polymer, wherein main chain scission takes place, leads to low-molecular weight polymer. (2) Crosslinking of small polymer units leads to the formation of a rigid three-dimensional network, wherein a high-

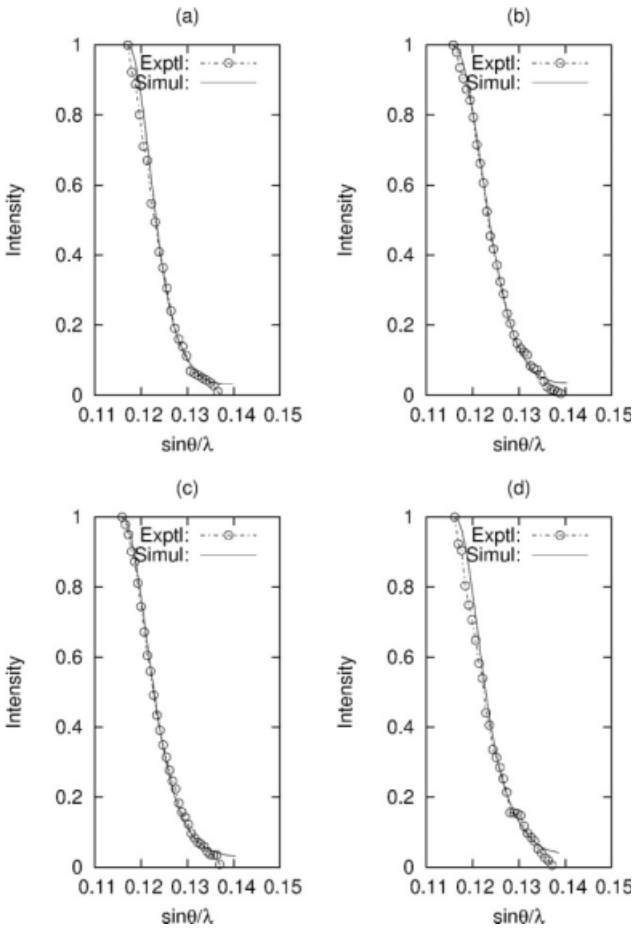

Figure 4 (a–d) Experimental and simulated intensity profiles of X-ray reflection of silk fiber samples obtained with Reinhold column length distribution function.

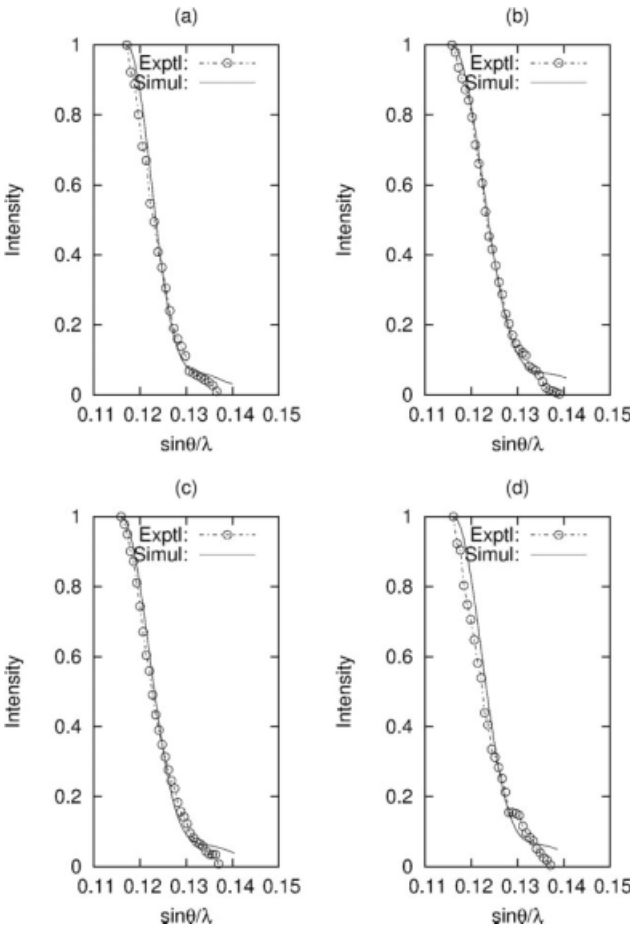

Figure 5 (a–d) Experimental and simulated intensity profiles of X-ray reflection of silk fiber samples obtained with lognormal column length distribution function.

molecular weight polymer is produced. Both these effects cause changes in physical properties. Degradation of polymer leads to loss in mechanical strength, whereas crosslinking improves the physical properties. It was found that the influence of electron beam irradiation, with increase in radiation dose and increase in degree of crosslinking results increase in modulus and T_g.[30] In the case of many other polymeric materials, ionizing radiation may crosslink them, which cause chain scission or affect their surface. Quite often these effects may occur simultaneously. The final result depends on the nature of the material, on the dosage, dosage rate, and energy of the radiation. From the Table II it is evident that the crystallite size decreases as irradiation dose increases. Normally the strength of the fibers, irrespective of natural or man-made, increases with increase in crystallite size.[31] This suggests that the unirradiated fiber is of more strength than the irradiated fibers. Our results clearly states that changes observed are due to degradation of the fiber sample.

The variation of lattice strain (g) lies between 0.3 and 0.6% in the case of exponential distribution for polymer samples. From the obtained micro crystalline parameters ($\langle N \rangle$, g in %) one can estimate the minimum enthalpy (α^*), which defines the equilibrium state of microparacrystals in all the polymer samples, using the relation postulated by Hosemann[32]

$$\alpha^* = (\langle N \rangle^{1/2} g) \tag{15}$$

The estimated minimum enthalpy is given in Table II. It is noted here that the value of α^* lies between 0.007 and 0.015 for these fiber samples. The value of enthalpy decreases with increasing dose rate which corresponds to the state with lower ordered polymer network. Energy for scission and for relaxation process in fibers is from the ion beam. The changes are inelastic and hence it takes a longer time to go back its original state. All this energy were observed at room temperature and hence one cannot expect by thermally changes imply for indicating such significant changes.[33] We have observed that the lattice strain and its variation for various values of the radiation doses (kGy) in polymer samples are very small and are almost insignificant.

CONCLUSIONS

From the wide-angle X-ray scattering (WAXS) study of electron irradiated C108 silk fiber (*Bombyx mori*) samples, we have observed that even though there is not much change in the position of the X-ray reflections, a significant change in the values of micro structural parameters occurs. The significant change in microstructural parameters in polymer is due to the effect of electron irradiation. This causes the degradation of small polymer units leading to the formation of low polymer network. We have shown that among the three asymmetric crystallite size distributions, exponential gives a better fit in polymer samples. The only justification for the good fit that we observed with exponential distribution in these polymers can be interpreted on the basis of extensive usage of this function in condensed matter to explain various phenomenon's like dielectric relaxation, luminescence decay law, and other physical properties. Single order method that we have used here is capable of estimating both the size and the distortion parameters and could in general measure crystallite size, only unto a certain limit. The changes in polymer network with different dose rates are quantified here in terms of microstructural parameters. Surprisingly we observed that the intrinsic strains are very small. It is evident from this study that irradiation of silk fibers changes

the polymer network and hence the physical properties.

References

1. Miller, L. D.; Putthanarat, S.; Adoms, W. W. Int J Biol Macromol 1999, 24, 159.
2. Mohanthy, N.; Das, H. K.; Mohanthy, P.; Mohanthy, E. J Macromol Sci A 1995, 32, 1103.
3. Kavahara, Y.; Shioya, M.; Takaku, A. J Appl Polym Sci 1996, 59, 51.
4. Freddi, G.; Massafra, M. R.; Beretta, S.; Shibata, S.; Gotch, Y.; Yasui, H.; Sukuda, M. T. J Appl Polym Sci 1996, 60, 11.
5. Tsukuda, M.; Freddi, G.; Monti, P. J Appl Polym Sci 1995, 33, 1995.
6. Tsukuda, M.; Obo, M.; Kato, H.; Freddi, G.; Zenetti, F. J Appl Polym Sci 1996, 60, 1619.
7. Tsukuda, M.; Gotch, Y.; Nagura, M.; Minoura, N.; Kasai, N.; Freddi, G. J Polym Sci Part B: Polym Phys 1994, 32, 961.
8. Somashekarappa, H.; Selvakumar, N.; Subramaniam, V.; Somashekar, R. J Appl Polym Sci 1996, 59, 1677.
9. Okuyama, K.; Takanashi, K.; Nakajima, Y.; Hasegawa, Y.; Hirabayashi, K.; Nishi, N. J Seric Sci 1988, 57, 23.
10. Somashekarappa, H.; Nadgir, G. S.; Somashekar, T. H.; Prabhu, J.; Somashekar, R. Polymer 1998, 39, 209.
11. Sangappa; Okuyama, K.; Somashekar, R. J Appl Polym Sci 2004, 91, 3045.
12. Sangappa; Mahesh, S. S.; Somashekar, R. J Biosci 2005, 30, 259.
13. Sangappa; Mahesh, S. S.; Somashekar, R.; Subramanya, G. J Polym Res 2005, 00, 1.
14. Takeshita, H.; Ishida, K.; Kamiishi, Y.; Yoshii, F.; Kume, T. Macromol Mater Eng 2000, 283, 126.
15. Kojthung, A.; Meesilpa, P.; Sudatis, B.; Treeratanapiboon, L.; Udomsangpetch, R.; Oonkhanond, B. Int Biodeterior Biodegrad 2008, 62, 487.
16. Wang, G.; Pao, G.; Dow, L.; Jiang, S.; Dai, Q. Nucl Instrum Methods B 1987, 27, 410.
17. Charlesky, A. J Polym Sci 1995, 15, 263.
18. Warren, B. E.; Averbach, B. L. J Appl Phys 1950, 21, 595.
19. Warren, B. E. Acta Crystallogr 1955, 8, 483.
20. Warren, B. E. X-ray Diffraction; Addision-Wesley: New York, 1969.
21. Hall, I. H.; Somashekar, R. J Appl Crystallogr 1991, 124, 105.
22. Ribarik, R.; Ungar, T.; Gubicza, J. J Appl Crystallogr 2001, 34, 669.
23. Popa, N. C.; Balzar, D. J Appl Crystallogr 1995, 35, 338.
24. Scardi, P.; Leoni, M. Acta Crystallogr Sect A 2001, 57, 604.
25. Balzar, D. IUCr Newslett 2002, 228, 14.
26. Somashekar, R.; Hall, I. H.; Carr, P. D. J Appl Crystallogr 1989, 22, 363.
27. Somashekar, R.; Somashekarappa, H. J Appl Crystallogr 1997, 130, 147.
28. Nandi, R. K.; Kho, H. K.; Schlosberg, W.; Wissler, G.; Cohen, J. B.; Crist, B., Jr. J Appl Crystallogr 1984, 17, 22.
29. Press, W.; Flannery, B. P.; Teukolsky, S.; Vetterling, W. T., Eds. Numerical Recipes; Cambridge University press: Cambridge, 1986.
30. Banik, I.; Bhowmick, A. K. Radiat Phys Chem 1999, 54, 135.
31. Lee, K. G.; Barton, R., Jr.; Schultz, J. M. J Polym Sci Part B: Polym Phys 1995, 33, 1.
32. Hosemann, R. Colloid Polym Sci 1982, 260, 864.
33. Klunzinger, P. E.; Eby, R. K. Polymer 1993, 34, 2431.